Published in final edited form as:
*Biomaterials*. 2011 March ; 32(9): 2417–2423. doi:10.1016/j.biomaterials.2010.11.071.

# The effect of biophysical attributes of the ocular trabecular meshwork associated with glaucoma on the cell response to therapeutic agents

**Clayton T. McKee**[1], **Joshua A. Wood**[1], **Nihar M. Shah**[1], **Marion E. Fischer**[1], **Christopher M. Reilly**[1,2], **Christopher J. Murphy**[1,3], and **Paul Russell**[1,*]

[1] Department of Surgical and Radiological Sciences, School of Veterinary Medicine, University of California Davis, Davis, USA

[2] Department of Pathology, Microbiology, and Immunology, School of Veterinary Medicine, University of California Davis, Davis, USA

[3] Department of Ophthalmology and Vision Science, School of Medicine, University of California Davis, Davis, USA

## Abstract

Glaucoma is a devastating neurodegenerative disease, which can lead to vision loss and is associated with irreversible damage to retinal ganglion cells. Although the mechanism of disease onset remains unknown, we have recently demonstrated that the stiffness of the ocular trabecular meshwork (HTM) increases dramatically in human donor eyes with a history of glaucoma. Here we report that polyacrylamide hydrogels, which mimic the compliant conditions of normal and glaucomatous HTM, profoundly modulate cytoskeletal dynamics and the elastic modulus of the overlying HTM cells. Substratum compliance also modulates HTM cell response to Latrunculin-B, a cytoskeletal disrupting agent currently in human clinical trials for the treatment of glaucoma. Additionally, we observed a compliance-dependent rebound effect of Latrunculin-B with an unexpected increase in HTM cell elastic modulus being observed upon withdrawal of the drug. The results predict that cytoskeletal disrupting drugs may be more potent in advanced stages of glaucoma.

## INTRODUCTION

Historically, laboratory investigations of cellular behaviors have been conducted on flat, rigid substrates such as glass or polystyrene. These substrates present cells with static, biophysical cues that differ greatly from those found in the human body. Within the body, cells interact with dynamic compliant environments that can change with aging [1,2] or during the progression of diseases such as cancer [3,4], atherosclerosis [5] and fibrosis [6]. Compliance of the substratum has also been shown to influence a wide range of fundamental cell behaviors including cell morphology [7,8], migration [7-10], proliferation [11,12] and differentiation [12-14].



*Corresponding Author. prussell@ucdavis.edu.

Recently, it has been reported that the compliance of the Human Trabecular Meshwork (HTM) is significantly *decreased* during the progression of glaucoma [15]. Glaucoma is a devastating neurodegenerative disease associated with irreversible damage of the optic nerve, which often leads to vision loss [16]. Although the mechanisms responsible for the onset of the disease remain unknown, glaucoma is commonly associated with increased IOP [17]. In humans, IOP is primarily maintained by outflow of aqueous humor through the trabecular meshwork [18-21] and is often elevated in patients with glaucoma, due to changes in the facility of aqueous outflow [22]. The results by Last et.al.,(15) suggest that the changes in stiffness of the HTM during the progression of glaucoma may influence the outflow facility of aqueous humor and therefore IOP. The HTM (Fig. 1) is a complex, three-dimensional structure comprised of trabecular meshwork cells and associated extracellular matrix comprised of interwoven collagen beams and perforated sheets [21]. The tissue reversibly deforms with normal physiological events such as accommodation and blinking [23,24] and therefore provides transient biophysical cues in the form of topography [25] and compliance [15], to human trabecular meshwork cells adhered within the meshwork.

In aggregate, findings on cellular response to substrate compliance suggest that alterations in meshwork compliance associated with glaucoma may also alter HTM cell physiology and subsequent response to therapeutic agents, which target the HTM to reduce IOP. Here, we report that alterations in substratum compliance that mimics the changes associated with glaucoma modulate the compliance of adhered HTM cells. Additionally, we present studies demonstrating that alterations in substratum compliance alter the response of HTM cells to drugs aimed at lowering IOP via disruption of the actin cytoskeleton.

All current clinical treatments for glaucoma attempt to slow the progression of the disease by lowering intraocular pressure [26], by either decreasing aqueous humor production or increasing aqueous humor outflow. Therapeutic compounds administered include beta blockers, prostaglandin analogues, alpha-adrenergic agonists, carbonic anhydrase inhibitors or a combination of these drugs [16]. Recently, Latrunculin B (Lat-B), a compound that induces reversible disruption of the actin cytoskeleton of cells [27], has been shown to increase aqueous humor outflow and decrease IOP [28-30]. Although disruption of the actin network has been proposed as the means by which IOP is lowered, changes in HTM architecture and mechanics that may regulate IOP have not been fully investigated. The immediate effect of Lat-B exposure on cell mechanics has been studied on a number of different cell types and results in a decrease in the elastic modulus of the cell by actin depolymerization [31,32]. Previous studies have been conducted on flat glass or plastic substrates with elastic moduli in the giga-pascal range. HTM cells never interact with substrates having such low compliance *in vivo*. The effect of substrate compliance on the mechanical response of a cell to Lat-B exposure has not been extensively investigated and the effect of substratum compliance on actin *repolymerization* and associated changes in cellular mechanics after exposure has not been defined. HTM cell recovery after exposure to Lat-B and the influence of substrate compliance are particularly important in the context of clinical treatment of glaucoma. A single application of Lat-B does not result in a long-term decrease in IOP, requiring repeated administration to maintain lowered IOP.

To better understand how HTM cells respond to and recover from Lat-B exposure in normal and glaucomatous trabecular meshwork, we have used an atomic force microscope (AFM) and fluorescence microscopy to study the disassembly and repolymerization of the actin cytoskeleton on polyacrylamide (PA) hydrogels that mimic the compliance of normal and glaucomatous HTM. Additionally, hard glass substrates were used to demonstrate how an extremely stiff surface, typical of standard cell culture substrates, could influence interpretation of data obtained from HTM cells.

# MATERIALS and METHODS

## HTM Cell Line and Fluorescent Staining Reagents

Primary HTM cells were obtained from corneal buttons from donors with no history of ocular diseases and that were not suitable for transplant. HTM cells were isolated as previously described[33], and cultured in DMEM/F12 (HyClone, Fisher Scientific, Waltham, MA) medium with 10% fetal bovine serum (Atlanta Biologicals, Lawrenceville, GA. All new primary cultures were incubated for four days with 0.1uM dexamethasone, and only cells that had increased expression of myocilin (a marker for HTM cell identity) were used for this study. All studies were conducted using cells before the $7^{th}$ passage. Normal HTM cells were employed because growth of HTM cells from glaucomatous individuals is generally not robust enough for cell culture experiments [34,35]. Cells were plated onto glass surfaces at 100,000 cells per surface. A similar number of cells were plated onto the biomimetic PA hydrogels. The cells were allowed to attach to the surfaces for 12 hours prior to the start of the experiment. Fluorescent images of the actin cytoskeleton were obtained from fixed cells stained with phalloidin-AlexaFluor 568 (Invitrogen, Carlsbad, CA). Fluorescent images of the cell membrane were obtained from live cells stained with wheat germ agglutinin-AlexaFluor 488 (Invitrogen).

## Biomimetic Polyacrylamide Hydrogel Synthesis

We have reported the average Young's modulus of the human trabecular meshwork to be 4.0±2.2 kPa for normal tissue and 80.0±32.5 kPa for glaucomatous tissue [15]. Using these values as a guide we prepared two different PA gels that mimicked the compliant conditions of normal (homeomimetic, HM) and glaucomatous (pathomimetic, PM) tissue. Polyacrylamide gels, formed by free-radical polymerization, have been widely used in the study of substrate compliance on cell behavior because the compliance can be easily tuned by altering the cross-linker density [7,14]. In addition, the surfaces of the PA gels can be functionalized to ensure cell adhesion and survival [7].

All pre-gel monomer solutions were prepared in 50 ml conical tubes. For the homeomimetic tissue polyacrylamide hydrogels (HM), 1.1 ml of a pre-mixed solution of acrylamide (Am) and N,N'-methylenebisacrylamide (BIS) (Am:BIS 29:1, 40%, Fisher Scientific), and 400 μl of (3-acrylamidepropyl)trimethylammonium chloride (API, 75% w/w, Sigma Aldrich, St. Louis, MO) were dissolved in 8.5 ml of ultrapure water (Millipore, Billerica, MA). To create pathomimetic substrates that approximate the compliance of glaucomatous meshwork (PM), an Am:BIS solution(18:1) was prepared by dissolving 3.554 g of Am (MP Biomedical, Solon, OH), 192.7 mg of BIS (Sigma), and 400 μl of API in 9.6 ml of ultrapure water. Dissolved oxygen is known to interfere with this type of free radical polymerization. The above solutions were kept at room temperature for one hour, prior to the addition of polymerization initiator and catalyst, to obtain repeatable results. Once equilibrated, 200 μl of 10% w/v solution of ammonium persulfate (Fisher Scientific) and 30 μl of tetramethylethylenediamine (Sigma) were added. These solutions were gently swirled in the conical tubes for 10-15 seconds and quickly poured into empty Criterion gel casting cassettes (1 mm thick, Bio-Rad, Hercules, CA). These containers are closed to the atmosphere except for a thin strip at the top of the cassette. After 60 minutes, the cassettes were cracked open, and substrates were cut using a 3/8 inch diameter round punch. The top centimeter of gels, closest to atmosphere, was discarded due to inconsistency in compliance values with the rest of the gel. To remove unreacted reagents, the cut PA gels were placed in polystyrene dishes and rinsed three times in 1x PBS (HyClone, Fisher Scientific). The gels were then sterilized in PBS with short wavelength (280 nm) UV light for 30 minutes. Finally, the PBS was replaced with fresh, sterile PBS and the substrates were stored in a $CO_2$ incubator at 37°C for at least 24 hours to attain their final equilibrium swelling.

The PA gels were then adhered to UV-cleaned, glass-bottom petri dishes (World Precision Instruments, Sarasota, FL), incubated in HTM medium for 12 hours, and then coated with a mixture of fibronectin and collagen (FNC coating mix, Athena Environmental Sciences, Baltimore, MD) for 10 minutes prior to cell seeding. HTM cells were added to these dishes in media and were allowed to incubate overnight to ensure proper cell adhesion to the FNC-coated PA gels. Immediately prior to AFM measurements, the HTM media was rinsed away with PBS. This was done because fetal bovine serum is known to inactivate Lat-B [36].

## Contact Mechanics

The contact mechanics of the PA substrates and the HTM cells were studied with two MFP-3D atomic force microscopes (Asylum Research, Santa Barbara, CA) interfaced with either an Olympus (FluoView 1000 laser scanning confocal microscope, Olympus America, Center Valley, PA) or Zeiss (Axio Observer A1, Carl Zeiss, Thornwood, NY) inverted microscope. No differences in contact mechanics of the samples were observed between the two instruments. The AFM probes in all of these studies were silicon nitride cantilevers (PNP-TR-50, $k$ = 60 pN/nm, NanoAndMore, Lady's Island, SC) with a square pyramid tip incorporated at the free end. For each experiment, the actual spring constant of the cantilever was determined by monitoring the amplitude of the lever's thermal vibration at resonance and applying the equipartition theorem [37]. All probe indentation measurements were obtained over the central region of the cell where the nucleus was present. Phase contrast imaging demonstrates alignment (Fig.2).

Compliance of the HTM cells and PA gels was quantified by fitting the force, generated by the indenting probe, vs. the depth of indentation with equation 1 [38].

$$F = \frac{2}{\pi} \tan(\alpha) \frac{E}{1-\nu^2} \delta^2 \qquad \text{Eq.1}$$

Where $\alpha$ is the half-angle opening of the square pyramid tip (35°), $\nu$ is Poisson's ratio, $E$ is Young's modulus and $\delta$ is the penetration depth. By using Eq.1, we have assumed that the HTM cells and PA gels were perfectly elastic, isotropic, and infinitely thick and that the square pyramid indenter was a rigid cone. A Poisson ratio of 0.5 (incompressible) for both the cell and polyacrylamide gels was assigned, since both samples were well hydrated. This allows a solution for Young's modulus of the sample.

Application of Eq. 1 is not straightforward, as both the cells and gels were not perfectly elastic or isotropic, they were viscoelastic and anisotropic, and they were also not infinitely thick. However, in the limit of small indentations both the cells and gels were well described by Eq.1. The method proposed by Mahaffey et al., [39] was applied to quantitatively define the indentation depth over which these viscoelastic materials behave as elastic bodies. This is accomplished by plotting experimental values of $E$ vs. $\delta$ during tip indentation and noting the penetration depth over which $E$ remains constant. In addition to defining the region of elastic response, defining the exact position of contact between the probe and cell or gel can introduce error in determining $E$. To help minimize this, very weak cantilever springs with manufacturers' spring constants of 60 pN/nm were used. Finally, many curves were averaged together to produce a mean and standard deviation force vs. indentation plots (Fig. 3). The main graph shows 25 different indentation vs. force curves (grey dots) measured at multiple positions on a PA gel. Contact was defined by visually noting where the cantilever deviates from a forward extrapolation of zero deflection. From these curves we generated a single curve of the average and two additional curves of the positive and negative standard deviations (black line with error bars, and open circles in the inset). A linear least-squares fit

of the data using Eq.1 (black lines) was then applied to the elastic region of these three curves to give an average and standard deviation of Young's modulus.

For each cell experiment, 5-7 cells were probed at ~2 um/s, with 5 indentation curves on each cell. Drive speeds were approximate due to the fact that the free end of cantilever slowed down once contact was made and the probe began to indent the sample. Young's modulus of the HTM cells was initially measured before Lat-B exposure. All force measurements were conducted in PBS. The cells were then exposed to a 0.2 uM Lat-B solution for 30 minutes. The concentration of Lat-B was based on previous studies examining the effects of lat-B on IOP [30]. At the end of this dose period, the Lat-B was rinsed away and the cells recovered in HTM medium. Young's modulus data were measured at 90 and 270 minutes (in PBS) post removal of Lat-B. All experiments were done in triplicate using primary HTM cells from three different donors.

## RESULTS

### Cell Morphology and Response to Exposure and Recovery from Latrunculin B

The morphology of HTM cells adhered to glass and the glaucomatous (pathomimetic) polyacrylamide gel (PM, 92.2±10.4 kPa) substrates were predominantly elongated with pronounced asymmetry. On the homeomimetic polyacrylamide gel (HM, 4.0±1.5 kPa), the cells were predominantly adhered in a radially symmetric fashion and were considerably rounder in appearance (Fig.5). When exposed to Lat-B, HTM cells on glass and PM substrates responded in a similar fashion to other cell types previously studied [27,32,40]. Lat-B disrupted the dynamic process of actin filament maintenance and the actin polymerization process rapidly shifted towards net depolymerization. Confocal imaging showed this resulted in a dramatic change in cell shape (Fig.4), demonstrating that actin filaments play a central role in HTM cell morphology. Figure 4 highlights an interesting finding observed with Lat-B treatment. The confocal fluorescent emission images were obtained before and at 30 minutes of exposure to Lat-B on glass by staining live cells with wheat germ agglutinin, a lectin that adheres to the cell membrane. As the cell retracted during drug treatment, it adhered to the glass with delicate processes. Z-stack images showed that these processes helped to anchor the retracting cell to the underlying glass. These strands resembled retraction fibers observed during mitosis[41]. Similar cable-like filaments have also been reported by Evanko et. al., [42]. A significant number of cells detached from the glass and HM substrates during subsequent rinsing steps, suggesting these were very weak adhesion points.

After rinsing the Lat-B from the dish, the cells very quickly began to repolymerize actin filaments, and they returned to their pre-exposure morphology within 60-90 minutes. The dramatic changes in cell morphology observed on glass and PM substrates were not as pronounced for HTM cells adhered to HM substrates as a result of exposure to, or recovery from Lat-B.

### Effect of Substrate Modulus on Cell Modulus Before and During Recovery From Latrunculin B

Prior to treatment with Lat-B, HTM cell compliance was proportional to the compliance of the underlying substrate. On glass with GPa modulus, Young's modulus of the HTM cells was 2.7±0.7 kPa. The elastic modulus of HTM cells grown on pathomimetic substrates was 1.8±0.5 kPa and was approximately 12% higher than cells grown on homeomimetic substrates 1.6±0.2 kPa (Table 1). Differences in compliance and cytoskeletal architecture between cells on pathomimetic and homeomimetic surfaces were also observed, and significantly more pronounced, upon recovery from Lat-B exposure. Fluorescent images of

the actin cytoskeleton confirmed that HTM cells on glass and the PM substrates produced significantly more actin stress fibers than cells adhered to the more compliant HM substrate (Fig.5). The greater degree of actin polymerization contributed to increased cell rigidity (increased Young's modulus). The fluorescent images also demonstrated HTM cells on the HM substrates were more rounded in appearance pre-dose and had fewer actin stress fibers. Loss of stress fibers with Lat-B exposure did not alter cell morphology as dramatically as the cells on the other two substrates.

The modulus of HTM cells at 30 minutes of Lat-B exposure was difficult to obtain, since the contracted cells offered almost no resistance to the indenting probe and the initial point of contact could not be reliably determined. However, when compared to pre-exposure levels, the cell resistance to deformation at 30 minutes of Lat-B exposure was substantially decreased. The primary observation for the response of HTM cells to Lat-B exposure and recovery is demonstrated in Figure 6 (on glass). During recovery, HTM cell modulus initially increased and then decreased back to pre-exposure levels by 270 minutes. For example, on glass, Young's modulus of the HTM cells before drug exposure was 2.8±0.5 kPa (circles). At 90 minutes after removal of Lat-B, the cell modulus increased to 10.1±2.4 kPa (squares) and then decreased back to 2.3±0.2 kPa (triangles) by 270 minutes of recovery. A similar trend was observed for both the PM and HM substrates. The magnitude of the differences in cell stiffness from before exposure and at 90 minutes of recovery increased proportional with substrate stiffness. Importantly, this trend was found at all time points, pre and post exposure to Lat-B, with a maximum percentage difference of approximately 54% (PM to HM) at 90 minutes of recovery. The combined results for HTM cells on glass and the compliant substrates mimicking glaucomatous and healthy tissue are shown in Table 1.

## DISCUSSION

### Relationship Between Cell Morphology and Modulus to Glaucoma

The actin cytoskeleton of HTM cells plays an important role in cell morphology and elastic modulus. As shown in Fig.4, polymeric actin, not intermediate filaments or tubulin, was the primary intracellular structure that maintained adhered HTM cell architecture. This actin network interfaces with the underlying substrate through focal adhesion complexes [43,44], and therefore the dynamic nature of HTM cell architecture and modulus was regulated, in part, by the biophysical cue of substrate compliance. As the elastic modulus of the substrate increased (became stiffer), the number of actin stress fibers within the cell increased, which led to an increased elastic modulus of the cell. This trend has also been reported for epithelial cells and fibroblasts on collagen coated PA gels [7] of varying stiffness. The elastic modulus of the HTM cells on our most rigid substrate, glass, was very similar to results found for endothelial cells from Schlemm's canal on rigid tissue culture polystyrene (TCP) dishes [45]. However, both glass and TCP have elastic modulus values in the GPa range. Such values are never present in the eye, and therefore present an unnatural biophysical cue to adhered cells, which stimulates actin polymerization. In addition, as the modulus of the substrate increased, the morphology of the cell changed from a rounded symmetric shape to an elongated asymmetric one. This is a clear indication that HTM cells are capable of detecting and responding to the changing extracellular biophysical cue of compliance associated with glaucoma.

### HTM cell response to exposure and removal of Latrunculin B

Substrate induced changes in the actin network of adhered HTM cells influenced the cell's response to Lat-B exposure. For both the glass and stiff (pathomimetic) polyacrylamide substrates, exposure to Lat-B induced dramatic changes in cell morphology due to disruption

of the more pronounced actin networks these cells contained. For HTM cells adhered to the very low modulus homeomimetic substrate, Lat-B had very little effect on cell morphology, due, at least in part, to the lesser amount of polymerized actin present within the cell prior to exposure. This finding suggests that the impact of treatment with Lat-B would be most pronounced in glaucomatous eyes possessing a stiffer meshwork. Additionally, topical application of Lat-B results in a wide array of cell types (e.g. corneal epithelial, stromal and endothelial cells, conjunctival cells) being exposed to the drug on its way to the meshwork. Cells adhered to very compliant substrates (e.g. corneal cells adhered to basement membranes with an elastic modulus of approximately 7.5 kPa [46]) would be affected to a much lesser degree than glaucomatous HTM cells attached to a much stiffer substrate. It also suggests that the impact of Lat-B on the actin network of “off target” cells could be affected by alteration in substratum compliance associated with disease states (e.g. fibrosis) and therapeutic interventions (e.g. corneal collagen cross-linking using riboflavin [47]).

The elastic modulus of HTM cells did not simply increase back to the observed compliant condition before exposure to Lat-B. During recovery, the elastic modulus of the cells initially increased above pre-dose values and then decreased back to a pre-dose elastic state by 270 minutes after Lat-B removal. Although this effect was observed for all three substrates, it was more pronounced on the substrates with the higher elastic modulus. The difference in cell elastic modulus between cells pre-exposure and cells at 90 minutes of recovery increased with increasing elastic modulus of the underlying substrate. As a control, the elastic modulus of HTM cells was additionally measured at 2, 4, 12, 24, and 120 hours from initial seeding, and no change in cell modulus was observed in the absence of exposure to Lat-B.

In both human and cynomolgus macaque eyes, application of Lat-B has been shown to increase aqueous outflow and lower IOP in glaucomatous eyes [29,30]. This demonstrates that the actin network of HTM cells plays a role in regulating IOP. Morphological changes in Lat-B treated eyes suggest that the increased outflow is due to an increased space between the inner wall of Schlemm's canal and the trabecular meshwork[48], termed the juxtacanalicular region (JXT). We have shown that disruption of actin stress fibers decreases the modulus of the HTM cells (i.e. a “softer” cell) and that this disruption is dependent on the disease state of the underlying substrate. These stress fibers influence the mechanical properties of the HTM through cell focal adhesions, which are capable of deforming compliant substrates[49,50]. The loss of cell-induced contractile loads upon exposure to Lat-B may therefore lead to the previously observed expansions of the JXT, by a concomitant softening of the HTM.

## CONCLUSION

Glaucoma is associated with alterations in the intrinsic biophysical attributes of the HTM. Changes in HTM compliance, in turn, are reflected by changes in HTM cell cytoskeletal dynamics. The relationship between substrate compliance and cell actin polymerization influences the response of HTM cells to the actin cytoskeleton-disrupting drug Latrunculin B. HTM cells were significantly more responsive to Lat-B when adhered to stiffer substrates due to the increased number of actin fibers, present before dose. As the meshwork stiffens, the adhered cells also stiffen due to increased actin stress fibers. Interestingly, there is a rebound effect of Lat-B application with an unexpected increase in cell modulus when the drug effect diminished. The modulus returned to pre-exposure levels in around four hours after this increase was observed. These data show the influence of substrate compliance on cellular compliance and response to therapeutic agents in relationship to disease states. The results have also led us to speculate on the mechanism by which Lat-B decreases IOP.

## Acknowledgments

The National Eye Institute IPA, 3UCD10-0076 and NIH, 1R01EY016134 funded this work.

## References

1. Lai-Fook SJ, Hyatt RE. Effects of age on elastic moduli of human lungs. J Appl Physiol 2000;89(1): 163–168. [PubMed: 10904048]
2. Erpelding TN, Hollman KW, O'Donnell M. Mapping age-related elasticity changes in porcine lenses using bubble-based acoustic radiation force. Exp Eye Res 2007;84(2):332–341. [PubMed: 17141220]
3. Samani A, Zubovits J, Plewes D. Elastic moduli of normal and pathological human breast tissues: an inversion-technique-based investigation of 169 samples. Phys Med Biol 2007;52(6):1565–1576. [PubMed: 17327649]
4. Krouskop TA, Wheeler TM, Kallel F, Garra BS, Hall T. Elastic moduli of breast and prostate tissues under compression. Ultrason Imaging 1998;20(4):260–274. [PubMed: 10197347]
5. Matsumoto T, Abe H, Ohashi T, Kato Y, Sato M. Local elastic modulus of atherosclerotic lesions of rabbit thoracic aortas measured by pipette aspiration method. Physiol Meas 2002;23(4):635–648. [PubMed: 12450265]
6. Yeh WC, Li PC, Jeng YM, Hsu HC, Kuo PL, Li ML, et al. Elastic modulus measurements of human liver and correlation with pathology. Ultrasound Med Biol 2002;28(4):467–474. [PubMed: 12049960]
7. Pelham RJ Jr. Wang Y. Cell locomotion and focal adhesions are regulated by substrate flexibility. Proc Natl Acad Sci U S A 1997;94(25):13661–13665. [PubMed: 9391082]
8. Isenberg BC, Dimilla PA, Walker M, Kim S, Wong JY. Vascular smooth muscle cell durotaxis depends on substrate stiffness gradient strength. Biophys J 2009;97(5):1313–1322. [PubMed: 19720019]
9. Chen CC, Hsieh PCH, Wang GM, Chen WC, Yeh ML. The influence of surface morphology and rigidity on the substrata on cell motility. Mater Lett 2009;63(21):1872–1875.
10. Wong JY, Velasco A, Rajagopalan P, Pham Q. Directed movement of vascular smooth muscle cells on gradient-compliant hydrogels. Langmuir 2003;19(5):1908–1913.
11. Liao SW, Yu TB, Guan Z. De novo design of saccharide-peptide hydrogels as synthetic scaffolds for tailored cell responses. J Am Chem Soc 2009;131(48):17638–17646. [PubMed: 19908839]
12. Leipzig ND, Shoichet MS. The effect of substrate stiffness on adult neural stem cell behavior. Biomaterials 2009;30(36):6867–6878. [PubMed: 19775749]
13. Banerjee A, Artha M, Choudhary S, Ashton RS, Bhatia SR, Schaffer DV, et al. The influence of hydrogel modulus on the proliferation and differnetiation of encapsulated neural stem cells. Biomaterials 2009;30(27):4695–4699. [PubMed: 19539367]
14. Discher DE, Janmey P, Wang YL. Tissue cells feel and respond to the stiffness of their substrate. Science 2005;310(5751):1139–1143. [PubMed: 16293750]
15. Last JA, Pan T, Ding Y, Reilly CM, Keller K, Acott TS, Fautsch MP, Murphy CJ, Russell P. Elastic modulus determination of normal and glaucomatous human trabecular meshwork. Invest Ophth Vis Sci. In Press.
16. Epstein, DL. Chandler and Grant's Glaucoma. 4th ed. Lippincott Williams & Wilkins; 1997.
17. Johnson M, Chan D, Read AT, Christensen C, Sit A, Ethier CR. The pore density in the inner wall endothelium of Schlemm's canal of glaucomatous eyes. Invest Ophth Vis Sci 2002;43(9):2950–2955.
18. Tamm ER. The trabecular meshwork outflow pathways: structural and functional aspects. Exp Eye Res 2009;88(4):648–655. [PubMed: 19239914]
19. Tektas OY, Lutjen-Drecoll E. Structural changes of the trabecular meshwork in different kinds of glaucoma. Exp Eye Res 2009;88(4):769–775. [PubMed: 19114037]
20. Overby DR, Stamer WD, Johnson M. The changing paradigm of outflow resistance generation: towards synergistic models of the JCT and inner wall endothelium. Exp Eye Res 2009;88(4):656–670. [PubMed: 19103197]

21. Johnson M. What controls aqueous humour outflow resistance? Exp Eye Res 2006;82(4):545–557. [PubMed: 16386733]
22. Grant WM. Clinical measurements of aqueous outflow. AMA Arch Ophthalmol 46(2):113–131. 195. [PubMed: 14856471]
23. Green K, Luxenberg MN. Consequences of eyelid squeezing on intra-ocular pressure. Am J Ophthalmol 1979;88(6):1072–1077. [PubMed: 517612]
24. Miller D. Pressure of lid on eye. Arch Ophthalmol 1967;78(3):328–&. [PubMed: 6040008]
25. Russell P, Gasiorowski JZ, Nealy PF, Murphy CJ. Response of human trabecular meshwork cells to topographic cues on the nanoscale level. Invest Ophth Vis Sci 2008;49(2):629–635.
26. Heijl A, Leske MC, Bengtsson B, Hyman L, Hussein M. Reduction of intraocular pressure and glaucoma progression: results from the early manifest glaucoma trial. Arch Ophthalmol 2002;120(10):1268–1279. [PubMed: 12365904]
27. Spector I, Shochet NR, Kashman Y, Groweiss A. Latrunculins: novel marine toxins that disrupt microfilament organization in cultured cells. Science 1983;219(4584):493–495. [PubMed: 6681676]
28. Tian B, Geiger B, Epstein DL, Kaufman PL. Cytoskeletal involvement in the regulation of aqueous humor outflow. Invest Ophth Vis Sci 2000;41(3):619–623.
29. Peterson JA, Tian B, Geiger B, Kaufman PL. Effect of latrunculin-B on outflow facility in monkeys. Exp Eye Res 2000;70(3):307–313. [PubMed: 10712817]
30. Ethier CR, Read AT, Chan DW. Effects of latrunculin-B on outflow facility and trabecular meshwork structure in human eyes. Invest Ophth Vis Sci 2006;47(5):1991–1998.
31. Radmacher M, Rotsch C. Drug-induced changes of cytoskeletal structure and mechanics in fibroblasts: An atomic force microscopy study. Biophys J 2000;78(1):520–535. [PubMed: 10620315]
32. Wakatsuki T, Schwab B, Thompson NC, Elson EL. Effects of cytochalasin D and latrunculin B on mechanical properties of cells. J Cell Sci 2001;114(5):1025–1036. [PubMed: 11181185]
33. Rhee DJ, Tamm ER, Russell P. Donor corneoscleral buttons: a new source of trabecular meshwork for research. Exp Eye Res 2003;77:749–746. [PubMed: 14609563]
34. Tschumper RC, Johnson DH. Trabecular meshwork cellularity-differences between fellow eyes. Invest Ophth Vis Sci 1990;31(7):1327–1331.
35. Gasiorowski JZ, Russell P. Biological properties of trabecular meshwork cells. Exp Eye Res 2009;88(4):671–675. [PubMed: 18789927]
36. Spector I, Shochet NR, Blasberger D, Kashman Y. Latrunculins--novel marine macrolides that disrupt microfilament organization and affect cell growth: I. Comparison with cytochalasin D. Cell Motil Cytoskel 1989;13(3):127–144.
37. Hutter JL, Bechhoefer J. Calibration of atomic force microscope tips. Rev Sci Instrum 1993;64(11):3342–3342.
38. Love AEH. Boussingesq's problem for a rigid cone. Q J Math 1939;10:161–175.
39. Mahaffy RE, Shih CK, MacKintosh FC, Kas J. Scanning probe-based frequency-dependent microrheology of polymer gels and biological cells. Phys Rev Lett 2000;85(4):880–883. [PubMed: 10991422]
40. Coue M, Brenner SL, Spector I, Korn ED. Inhibition of actin polymerization by latrunculin-A. Febs Lett 1987;213(2):316–318. [PubMed: 3556584]
41. Sanger JM, Reingold AM, Sanger JW. Cell surface changes during mitosis and cytokinesis of epithelial cells. Cell Tissue Res 1984;237(3):409–417. [PubMed: 6488284]
42. Evanko SP, Potter-Perigo S, Johnson PY, Wight TN. Organization of hyaluronan and versican in the extracellular matrix of human fibroblasts treated with the viral mimetic poly I:C. J Histochem Cytochem 2009;57(11):1041–1060. [PubMed: 19581629]
43. Lazarides E, Burridge K. Alpha-actinin: immunofluorescent localization of a muscle structural protein in nonmuscle cells. Cell 1975;6(3):289–298. [PubMed: 802682]
44. Burridge K, Chrzanowska-Wodnicka M. Focal adhesions, contractility, and signaling. Annu Rev Cell Dev Biol 1996;12:463–518. [PubMed: 8970735]

45. Zeng D, Juzkiw T, Read AT, Chan DW, Glucksberg MR, Ethier CR, et al. Young's modulus of elasticity of Schlemm's canal endothelial cells. Biomech Model Mechanobiol 2010;9(1):19–33. [PubMed: 19387710]

46. Last JA, Liliensiek SJ, Nealey PF, Murphy CJ. Determining the mechanical properties of human corneal basement membranes with atomic force microscopy. J Struct Biol 2009;167(1):19–24. [PubMed: 19341800]

47. Kymionis G, Portaliou D. Corneal crosslinking with riboflavin and UVA for the treatment of keratoconus. J Cataract Refr Surg 2007;33(7):1143–1144.

48. Sabanay I, Tian B, Gabelt BT, Geiger B, Kaufman PL. Latrunculin B effects on trabecular meshwork and corneal endothelial morphology in monkeys. Exp Eye Res 2006;82(2):236–246. [PubMed: 16054137]

49. Harris AK, Wild P, Stopak D. Silicone rubber substrata: a new wrinkle in the study of cell locomotion. Science 1980;208(4440):177–179. [PubMed: 6987736]

50. Burridge K. Are stress fibres contractile? Nature 1981;294(5843):691–692. [PubMed: 7198718]

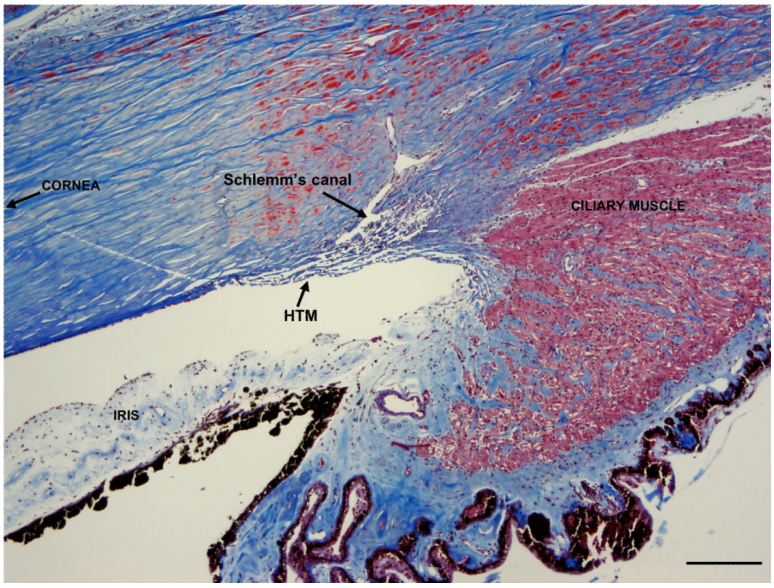


**FIGURE 1.**

Human Trabecular Meshwork. The HTM is located at the inner corneoscleral junction, near the base of the iris. It is composed of collagen beams (blue) lined by trabecular meshwork cells forming a 3-dimensional “sieve”-like network. This structure is responsible for determining outflow facility, as it directly abuts Schlemm's canal. Ciliary muscle fibers (stained red) insert on the posterior aspect of the meshwork. Masson's trichrome stain, scale bar 200 μm.

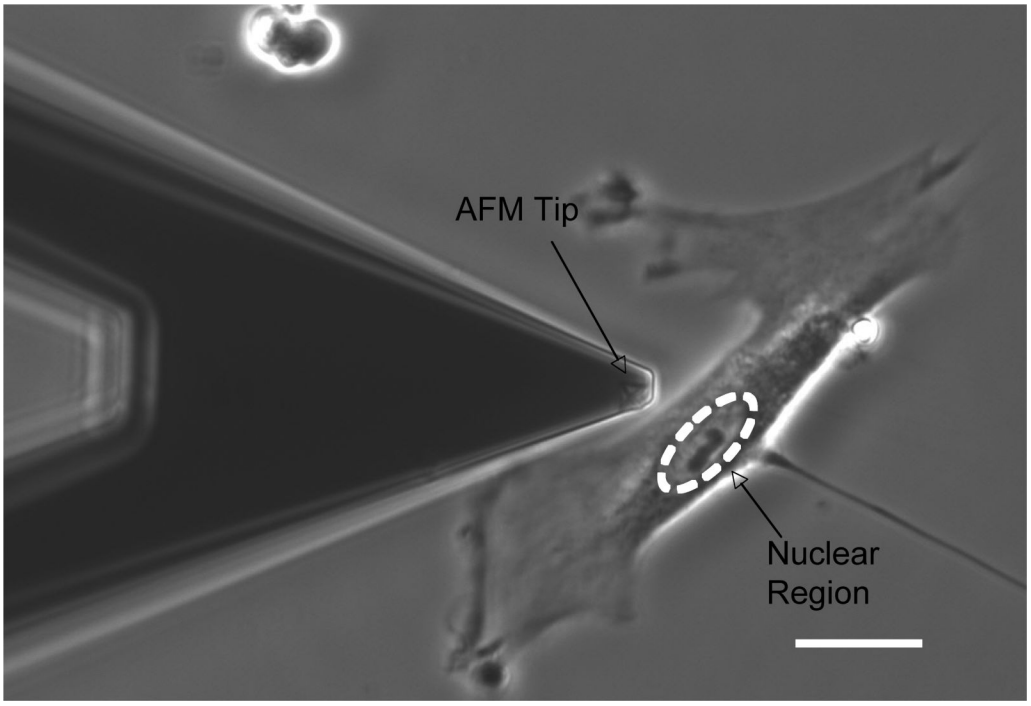


**FIGURE 2.**
Phase image demonstrating how an AFM tip (x pattern at end of tip) can be aligned over nuclear region of cell. Scale bar 20 μm.

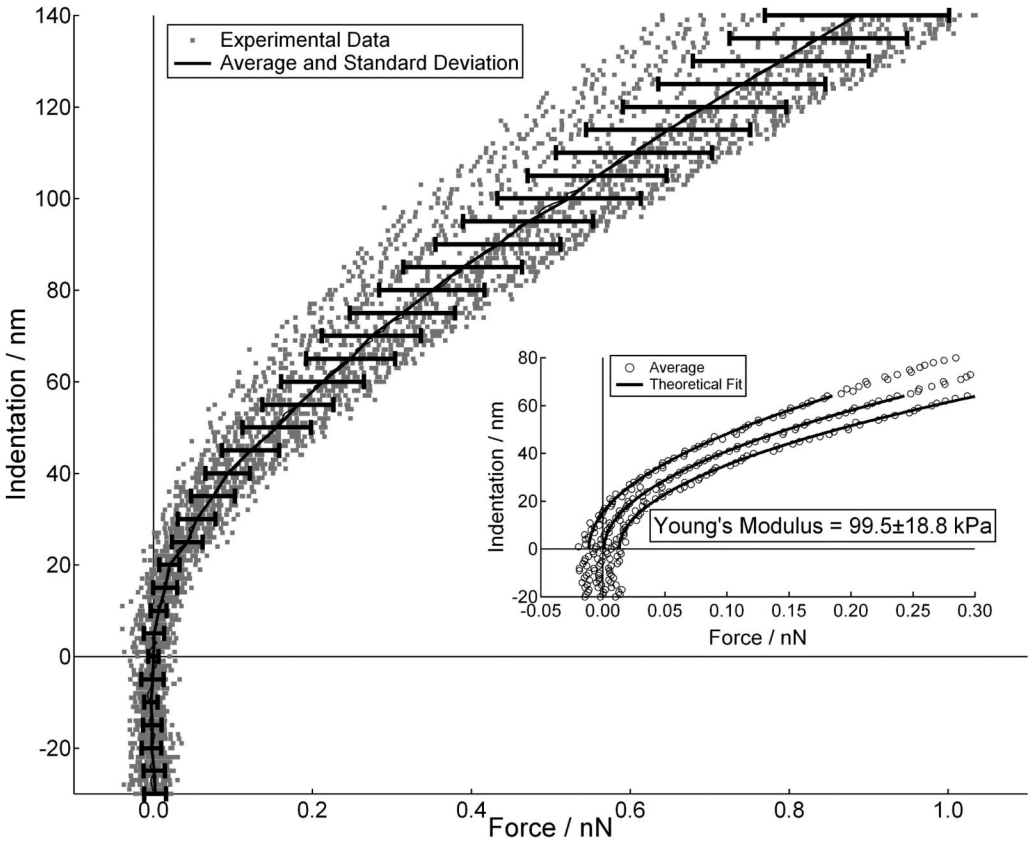


**FIGURE 3.**

Indentation vs. force curves measured at 5 different positions on a polyacrylamide gel. At each position 5 force curves were measured (grey dots). The average and standard deviation of these 25 curves overlays the data (black lines). The inset is a plot of the average and the positive and negative standard deviation curves. The solid lines in the inset are linear least square fits of the average and standard deviation curves, which gave a result of 99.5±18.8 kPa.

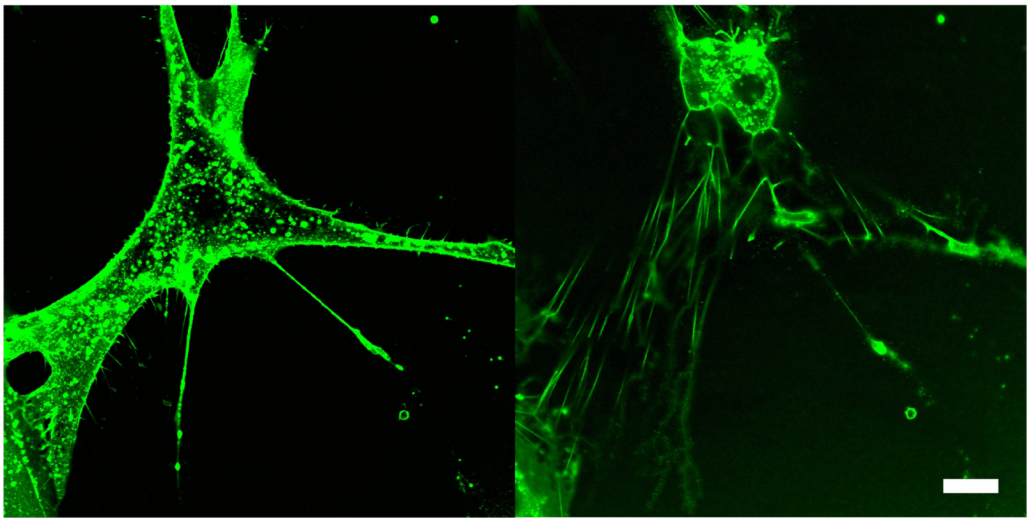

**FIGURE 4.**

Confocal images of a live HTM cell adhered to glass, before (left) and 30 minutes after exposure to Lat-B (right). Cell membrane was stained with fluorescent wheat germ agglutinin. During collapse of the cell body, delicate retraction fibers coated in WGA, maintain adhesion with underlying substrate. Scale bar 20 μm.

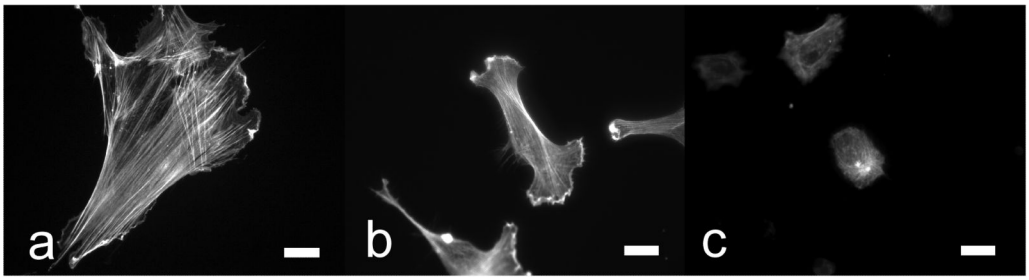


**FIGURE 5.**
Fluorescent images of the Actin network of HTM cells adhered to glass (a), PM (b) and HM (c) substrates. Scale bar 20 μm.

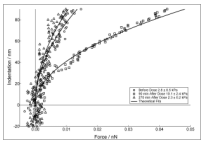

**FIGURE 6.**

Indentation vs. force curves measured on HTM cells on glass before dose (circles), and 90 and 270 minutes after exposure and removal of Lat-B (squares and triangles respectively). HTM cell resistance to deformation increased ~ 4 times at 90 minutes, and then decreased back to the pre-dosed cell modulus within 270 minutes of exposure.

## TABLE 1

HTM Cell modulus before exposure to Latrunculin B, and 90 and 270 minutes after exposure and removal of Latrunculin B. Cell modulus on both glass and pathomimetic substrate was significantly increased at 90 minutes of actin repolymerization. Within 270 minutes, cells have returned to pre-dose modulus values.

**HTM Cell Modulus on Substrates (kPa)**

| Condition | Glass[1] | Pathomimetic[2] | Homeomimetic[3] |
|---|---|---|---|
| Pre-dose | 2.7±0.7 | 1.8±0.5 | 1.6±0.2 |
| 90 min. rec. | 11.0±2.3 | 4.0±1.8 | 2.3±0.2 |
| 270 min. rec. | 2.3±0.2 | 2.0±0.4 | 1.7±0.5 |

[1] Elastic modulus, *E*, in GPa range

[2] $E$ = 92±10 kPa

[3] $E$ = 4.0±1.5 kPa